SLAC-PUB-10241

October 2003

Study of *CP* Asymmetries in Charmless Hadronic B Decays: Toward a measurement of α

James D. Olsen (Representing the *BABAR* Collaboration) [a]

[a]Department of Physics, Princeton University
Princeton, NJ, 08544

We present preliminary measurements of time-dependent *CP* asymmetries in neutral B meson decays to $\pi^+\pi^-$ and $\pi^+\pi^-\pi^0$ final states, where the latter is measured in the region of the Dalitz plane dominated by the ρ resonance. We also present preliminary measurements of the branching fraction for the decay $B^+ \to \pi^+\pi^0$ and an improved upper limit for $B^0 \to \pi^0\pi^0$, both of which are needed to extract the *CP* parameter α from the time-dependent *CP* asymmetry in the $\pi^+\pi^-$ channel. These results are obtained from a data sample of approximately 88 million $\Upsilon(4S) \to B\overline{B}$ decays collected with the *BABAR* detector at the PEP-II asymmetric-energy B Factory at SLAC.

1. Introduction

The Standard Model of electroweak interactions describes *CP* violation as a consequence of a single complex phase in the three-generation Cabibbo-Kobayashi-Maskawa (CKM) quark-mixing matrix [1]. The agreement between the direct measurements of the *CP* parameter sin2β reported at this conference [2,3], and the Standard Model prediction based on indirect constraints on the magnitudes of the elements of the CKM matrix, is strong evidence that the Kobayashi-Maskawa mechanism is the dominant source of *CP* violation in flavor-changing processes. One of the primary goals of the B-Factory experiments in the future will be to measure the remaining angles (α and γ) of the Unitarity Triangle in order to further test whether the Standard Model description of *CP* violation is correct.

In B decays to $\pi^+\pi^-$ and $\pi^+\pi^-\pi^0$ final states, the time-dependent *CP* asymmetry is related to the angle $\alpha \equiv \arg\left[-V_{\rm td}V_{\rm tb}^*/V_{\rm ud}V_{\rm ub}^*\right]$. The final state $\pi^+\pi^-$ is a *CP* eigenstate and the decay rate distribution $f_+\,(f_-)$ when the second B meson ($B_{\rm tag}$) is identified as a $B^0\,(\overline{B}^0)$ is given by [4]

$$f_\pm(\Delta t) = \frac{e^{-|\Delta t|/\tau}}{4\tau}[1 \quad \pm \quad S_{\pi\pi}\sin(\Delta m_d \Delta t) \quad \mp \quad C_{\pi\pi}\cos(\Delta m_d \Delta t)], \quad (1)$$

where τ is the mean B^0 lifetime, Δm_d is the mixing frequency due to the eigenstate mass difference, and Δt is the difference in proper decay times between the reconstructed meson and the tagging meson $B_{\rm tag}$. The parameters $S_{\pi\pi}$ and $C_{\pi\pi}$ are defined as

$$S_{\pi\pi} \equiv \frac{2\,\mathcal{I}m\lambda}{1+|\lambda|^2} \quad \text{and} \quad C_{\pi\pi} \equiv \frac{1-|\lambda|^2}{1+|\lambda|^2}, \quad (2)$$

and vanish in the absence of *CP* violation. If the decay proceeds purely through the $b \to u$ tree amplitude, the complex parameter λ is given by

$$\lambda(B \to \pi^+\pi^-) = \left(\frac{V_{\rm tb}^* V_{\rm td}}{V_{\rm tb} V_{\rm td}^*}\right)\left(\frac{V_{\rm ud}^* V_{\rm ub}}{V_{\rm ud} V_{\rm ub}^*}\right). \quad (3)$$

In this case $C_{\pi\pi} = 0$ and $S_{\pi\pi} = \sin 2\alpha$. In general, the $b \to d$ gluonic penguin amplitude modifies both the magnitude and phase of λ, so that $C_{\pi\pi} \neq 0$ and $S_{\pi\pi} = \sqrt{1-C_{\pi\pi}^2}\sin 2\alpha_{\rm eff}$, where $\alpha_{\rm eff}$ depends on the magnitudes and relative strong and weak phases of the tree and penguin amplitudes. In this case, measurements of the branching fractions for the decays $B^+ \to \pi^+\pi^0$ and $B^0 \to \pi^0\pi^0$ can be used to extract α from a measurement of $\alpha_{\rm eff}$ [5,6].

Since the final state $\rho^+\pi^-$ is not a *CP* eigenstate, four possible decay paths must be considered: $B^0(\overline{B}^0) \to \rho^\pm\pi^\mp$. In this case, the decay

Work supported in part by the Department of Energy contract DE-AC03-76SF00515.
Stanford Linear Accelerator Center, Stanford University, Stanford, CA 94309
Contributed to the 31st International Conference on High Energy Physics (ICHEP 2002), 7/24/2002 - 7/31/2002, Amsterdam, The Netherlands

Table 1
Average tagging efficiency ϵ, average mistag fraction w, mistag fraction difference $\Delta w = w(B^0) - w(\overline{B}^0)$, and effective tagging efficiency $Q = \epsilon(1-2w)^2$ for signal events in each tagging category. The quantities are measured in the $B_{\rm flav}$ sample.

Category	ϵ (%)	w (%)	Δw (%)	Q (%)
`Lepton`	9.1 ± 0.2	3.3 ± 0.7	-1.6 ± 1.3	8.0 ± 0.3
`Kaon I`	16.6 ± 0.2	9.5 ± 0.7	-2.8 ± 1.3	10.7 ± 0.4
`Kaon II`	19.8 ± 0.3	20.6 ± 0.8	-5.3 ± 1.3	6.7 ± 0.4
`Inclusive`	20.1 ± 0.3	31.7 ± 0.9	-2.6 ± 1.4	2.7 ± 0.3
`Untagged`	34.4 ± 0.5			
Total Q				28.4 ± 0.7

rate distributions can be written as [7]

$$f_T^{\rho^\pm\pi^\mp}(\Delta t) = (1 \pm A_{CP}^{\rho\pi})\frac{e^{-|\Delta t|/\tau}}{4\tau}[1 + T((S_{\rho\pi} \pm \Delta S_{\rho\pi})\sin(\Delta m_d \Delta t) - (C_{\rho\pi} \pm \Delta C_{\rho\pi})\cos(\Delta m_d \Delta t))], \quad (4)$$

where T indicates the flavor of $B_{\rm tag}$ ($B^0 = +1$, $\overline{B}^0 = -1$). The parameters $S_{\rho\pi}$ and $C_{\rho\pi}$ are analogous to $S_{\pi\pi}$ and $C_{\pi\pi}$ and are sensitive to α and direct CP violation, respectively. The time-integrated asymmetry $A_{CP}^{\rho\pi} \equiv \left[N_{\rho^+\pi^-} - N_{\rho^-\pi^+}\right] / \left[N_{\rho^+\pi^-} + N_{\rho^+\pi^-}\right]$ also measures direct CP violation, but independent of the flavor of $B_{\rm tag}$. The parameters $\Delta C_{\rho\pi}$ and $\Delta S_{\rho\pi}$ are intrinsically CP invariant. The asymmetry between $N(B^0_{\rho\pi} \to \rho^+\pi^-) + N(\overline{B}^0_{\rho\pi} \to \rho^-\pi^+)$ and $N(B^0_{\rho\pi} \to \rho^-\pi^+) + N(\overline{B}^0_{\rho\pi} \to \rho^+\pi^-)$ is described by $\Delta C_{\rho\pi}$, while $\Delta S_{\rho\pi}$ is sensitive to the strong phase difference between the amplitudes contributing to $B^0 \to \rho\pi$ decays.

The results reported here are described in more detail in separate papers [8] submitted to this conference.

2. Common Analysis Issues

At the $\Upsilon(4S)$, $B\overline{B}$ events can be distinguished from continuum $q\bar{q}$ production using two kinematic variables, the difference ΔE between the center-of-mass (CM) energy of the B meson candidate and $\sqrt{s}/2$, and the beam-energy substituted mass $m_{\rm ES} = \sqrt{(s/2 + \mathbf{p}_i \cdot \mathbf{p}_B)^2/E_i^2 - \mathbf{p}_B^2}$, where $\sqrt{s}$ is the total CM energy, and the B momentum $\mathbf{p_B}$ and the four-momentum of the initial state $(E_i, \mathbf{p_i})$ are defined in the laboratory frame. For signal decays $m_{\rm ES}$ peaks near the B mass and ΔE peaks near zero when the correct mass hypothesis is assigned to all daughter particles. When there is ambiguity, as in the decay $B^0 \to h^+h^-$ with $h = \pi$ or K, we use the pion mass when calculating four-momenta, which results in a shift of $-45\,$MeV in ΔE for each kaon in the decay.

Identification of charged tracks as pions or kaons is accomplished with the Cherenkov angle measurement θ_c from a detector of internally reflected Cherenkov light [9]. We use the information on θ_c directly in our maximum likelihood fits, which allows simultaneous measurement of $\pi^+(\pi^-/K^-)$, $\pi^0(\pi^+/K^+)$, and $\rho^+(\pi^-/K^-)$ decays. The typical separation between pions and kaons varies from $8\sigma_{\theta_c}$ at $2\,{\rm GeV}/c$ to $2.5\sigma_{\theta_c}$ at $4\,{\rm GeV}/c$.

The dominant background to charmless B decays is from the process $e^+e^- \to q\bar{q}$ ($q = u, d, s, c$). To suppress this background, we use multivariate techniques that discriminate between the jet-like topology of $q\bar{q}$ events and the more spherical topology of $B\overline{B}$ events. For the analysis of $\pi^+\pi^-\pi^0$ decays we use a neural network, while the remaining analyses use a Fisher discriminant.

We use a multivariate technique [2] to determine the flavor of the $B_{\rm tag}$ meson. Separate neural networks are trained to identify primary

leptons, kaons, soft pions from D^* decays, and high-momentum charged particles from B decays. Events are assigned to one of five mutually exclusive tagging categories based on the estimated mistag probability and the source of the tagging information. Table 1 summarizes the tagging performance measured in a data sample $B_{\rm flav}$ of fully reconstructed neutral B decays to $D^{(*)-}(\pi^+,\, \rho^+,\, a_1^+)$.

The time difference Δt is obtained from the known boost of the e^+e^- system and the measured distance between the z positions of the B candidate and the $B_{\rm tag}$ decay vertices. A detailed description of the algorithm is given in Ref. [10]. We determine the parameters of the signal resolution function from a fit to the $B_{\rm flav}$ sample (including events in all five tagging categories), while the form of the background Δt distribution is obtained from a signal-free region in data.

3. Analysis of $B^0 \to \pi^+\pi^-$

We analyze the decays $B^0 \to \pi^+\pi^-$, $K^+\pi^-$, K^+K^- simultaneously. Event yields are obtained from an unbinned extended maximum likelihood fit using $m_{\rm ES}$, ΔE, the Fisher discriminant, and θ_c measurements for each track. We include separate components for $K^+\pi^-$ and $K^-\pi^+$ in order to measure the direct CP asymmetry $\mathcal{A}_{CP}^{K\pi}$. The parameters of the background PDFs are obtained directly from the data, while signal parameters are determined from a mix of GEANT4 Monte Carlo simulation and control samples in data. Figure 1 shows distributions of $m_{\rm ES}$ and ΔE for subsamples of events enriched in $\pi\pi$ and $K\pi$ decays using probability ratios. The results are summarized in Table 2. The dominant sources of systematic error on the branching fraction measurements are from uncertainty in track and θ_c reconstruction efficiencies and imperfect knowledge of the PDF shapes. For $\mathcal{A}_{CP}^{K\pi}$ the systematic error is dominated by the θ_c PDF shape and possible charge bias in track reconstruction.

The parameters $S_{\pi\pi}$ and $C_{\pi\pi}$ are obtained from a second fit including tagging and Δt information. The Δt PDF for signal $\pi^+\pi^-$ decays is given by Eq. 1, modified to include w_k and Δw_k for each tagging category and convolved with the

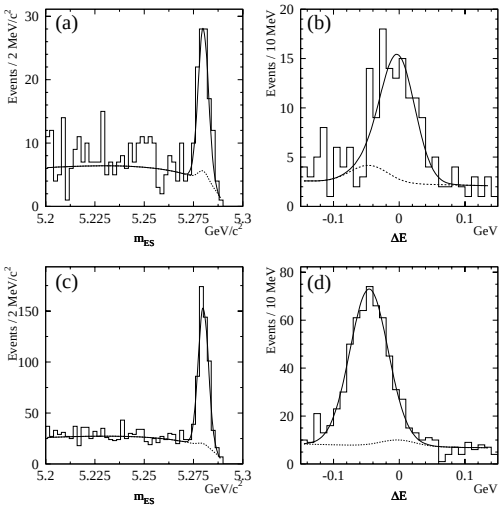

Figure 1. Distributions of $m_{\rm ES}$ and ΔE for events enhanced in signal (a), (b) $\pi^+\pi^-$ and (c), (d) $K^\mp\pi^\pm$ decays. Solid curves represent projections of the maximum likelihood fit, dashed curves represent $q\bar{q}$ and $\pi\pi \leftrightarrow K\pi$ cross-feed background.

signal resolution function. The Δt PDF for signal $K^+\pi^-$ events takes into account B^0–$\overline{B}^0$ mixing based on the charge of the kaon and the flavor of $B_{\rm tag}$. As a means of validating the analysis technique, we determine τ and Δm_d using signal $\pi^+\pi^-$ and $K^+\pi^-$ decays and find $\tau = (1.56 \pm 0.07)\,{\rm ps}$ and $\Delta m_d = (0.52 \pm 0.05)\,{\rm ps}^{-1}$. The fit yields

$$\begin{aligned} S_{\pi\pi} &= 0.02 \pm 0.34\,({\rm stat}) \pm 0.05\,({\rm syst}) \\ C_{\pi\pi} &= -0.30 \pm 0.25\,({\rm stat}) \pm 0.04\,({\rm syst}), \end{aligned}$$

where the correlation between $S_{\pi\pi}$ and $C_{\pi\pi}$ is -10%. Systematic uncertainties on $S_{\pi\pi}$ and $C_{\pi\pi}$ are dominated by imperfect knowledge of the PDF shapes and possible fit bias. Figure 2 shows distributions of Δt for events with $B_{\rm tag}$ tagged as B^0 or $\overline{B}^0$, and the asymmetry as a function of Δt for tagged events enhanced in signal $\pi\pi$ decays. We find no evidence for large mixing-induced, or direct CP violation, as reported in [13].

Table 2
Summary of results for total detection efficiencies, fitted signal yields N_S, charge-averaged branching fractions $\mathcal{B}$, and CP asymmetries $\mathcal{A}_{CP} \equiv [N_{\overline{B}^0} - N_{B^0}]/[N_{\overline{B}^0} + N_{B^0}]$ for various charmless two-body B decays. Branching fractions are calculated assuming equal rates for $\Upsilon(4S) \to B^0\overline{B}^0$ and B^+B^-. The upper limit yields and branching fractions for $\pi^+\pi^0$ and K^+K^- correspond to the 90% C.L. All results are consistent with similar measurements from other experiments [11].

Mode	Efficiency (%)	N_S	$\mathcal{B}(10^{-6})$	$\mathcal{A}_{CP}$
$\pi^+\pi^-$	38.0 ± 0.8	$157 \pm 19 \pm 7$	$4.7 \pm 0.6 \pm 0.2$	
$\pi^+\pi^0$	26.1 ± 1.7	$125^{+23}_{-21} \pm 10$	$5.5^{+1.0}_{-0.9} \pm 0.6$	$-0.03^{+0.18}_{-0.17} \pm 0.02$
$\pi^0\pi^0$	16.5 ± 1.7	23^{+10}_{-9} (< 46)	< 3.6	
$K^+\pi^-$	37.5 ± 0.8	$589 \pm 30 \pm 17$	$17.9 \pm 0.9 \pm 0.7$	$-0.102 \pm 0.050 \pm 0.016$
$K^+\pi^0$	21.5 ± 1.5	$239^{+21}_{-22} \pm 6$	$12.8^{+1.2}_{-1.1} \pm 1.0$	$-0.09 \pm 0.09 \pm 0.01$
K^+K^-	36.2 ± 0.8	1 ± 8 (< 16)	< 0.6	

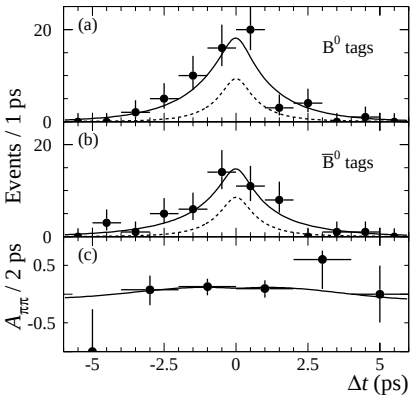

Figure 2. Distributions of Δt for events enhanced in signal $\pi\pi$ decays with $B_{\rm tag}$ tagged as (a) B^0 (N_{B^0}) or (b) $\overline{B}^0$ ($N_{\overline{B}^0}$), and (c) the asymmetry $\left[N_{B^0} - N_{\overline{B}^0}\right] / \left[N_{B^0} + N_{\overline{B}^0}\right]$ as a function of Δt. Solid curves represent projections of the maximum likelihood fit, dashed curves represent the sum of $q\bar{q}$ and $K\pi$ background events.

3.1. Constraining $|\alpha_{\rm eff} - \alpha|$

The isospin relationship between the final states $\pi^+\pi^-$, $\pi^+\pi^0$, and $\pi^0\pi^0$ allows the determination of α given a measurement of $\alpha_{\rm eff}$. Assuming isospin invariance, the shift in α is bounded by the relation $\sin^2(\alpha_{\rm eff} - \alpha) < \mathcal{B}(B^0 \to \pi^0\pi^0)/\mathcal{B}(B^+ \to \pi^+\pi^0)$ [6], where the branching fractions are averaged over $B^0/\overline{B}^0$ and B^+/B^-. Details of the branching fraction measurements are reported elsewhere [8], and summarized in Table 2. Including correlations and systematic errors, we find $BR(B^0 \to \pi^0\pi^0)/\mathcal{B}(B^+ \to \pi^+\pi^0) < 0.61$ at 90% C.L., which corresponds to $|\alpha_{\rm eff} - \alpha| < 51^\circ$.

4. Analysis of $B^0 \to \rho^+\pi^-$

A clean determination of α from the decay $B^0 \to \pi^+\pi^-\pi^0$ can only be accomplished with a full Dalitz analysis, including resonant and non-resonant contributions. However, a full analysis requires significantly more data than is currently available. We therefore restrict ourselves in this analysis to the regions of the Dalitz plane dominated by the ρ resonance, and we analyze $\rho\pi$ and ρK decays simultaneously.

Due to the presence of a neutral pion, there is a significant background from other B decay modes which can fake the $\rho\pi$ final state. We have investigated more than 80 decay modes and identified 20 charmless decays which have more than one event entering the final sample. These decays are parameterized and included in the maximum likelihood fit. We also include contributions from misreconstructed signal events and continuum $q\bar{q}$ background.

The fit technique is similar to the one used in the $\pi^+\pi^-$ analysis. We find 413^{+34}_{-33} $\rho\pi$ and 147^{+22}_{-21} ρK candidates and measure the following

CP parameters

$$
\begin{aligned}
S_{\rho\pi} &= 0.16 \pm 0.25\,(\text{stat}) \pm 0.07\,(\text{syst}),\\
C_{\rho\pi} &= 0.45^{+0.18}_{-0.19}\,(\text{stat}) \pm 0.09\,(\text{syst}),\\
A^{\rho\pi}_{CP} &= -0.22 \pm 0.08\,(\text{stat}) \pm 0.07\,(\text{syst}),\\
A^{\rho K}_{CP} &= 0.19 \pm 0.15\,(\text{stat}) \pm 0.11\,(\text{syst}),
\end{aligned}
$$

and the *CP* invariant quantities

$$
\begin{aligned}
\Delta S_{\rho\pi} &= 0.15 \pm 0.26\,(\text{stat}) \pm 0.05\,(\text{syst}),\\
\Delta C_{\rho\pi} &= 0.38^{+0.19}_{-0.20}\,(\text{stat}) \pm 0.11\,(\text{syst}).
\end{aligned}
$$

The dominant source of systematic error in this analysis is from uncertainty in the level of background from other B decays, and in the parameterization of the PDFs for those decays. Figure 3 shows distributions of Δt for events with $B_{\rm tag}$ tagged as B^0 or $\overline{B}^0$, and the asymmetry as a function of Δt for tagged events enhanced in signal $\rho\pi$ decays.

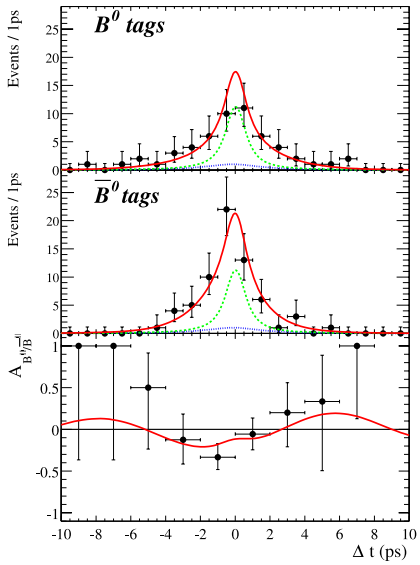

Figure 3. Distributions of Δt for events enhanced in signal $\rho\pi$ decays with $B_{\rm tag}$ tagged as (a) B^0 (N_{B^0}) or (b) $\overline{B}^0$ ($N_{\overline{B}^0}$), and (c) the asymmetry $\left[N_{B^0} - N_{\overline{B}^0}\right] / \left[N_{B^0} + N_{\overline{B}^0}\right]$ as a function of Δt. Solid curves represent projections of the maximum likelihood fit, dotted curves represent backgrounds from $B\overline{B}$ events, and dashed curves represent the sum of $q\bar{q}$ and $B\overline{B}$ background events.

REFERENCES

1. N. Cabibbo, Phys. Rev. Lett. **10**, 531 (1963); M. Kobayashi and T. Maskawa, Prog. Th. Phys. **49**, 652 (1973).
2. *BABAR* Collaboration, B. Aubert *et al.*, SLAC-PUB-9293, hep-ex/0207042, to appear in Phys. Rev. Lett.
3. BELLE Collaboration, K. Abe *et al.*, hep-ex/0208025, submitted to Phys. Rev. D **.**
4. For a general review of the formalism see Y. Nir and H. Quinn, Ann. Rev. Nucl. Part. Sci. **42**, 211 (1992).
5. M. Gronau and D. London, Phys. Rev. Lett. **65**, 3381 (1990).
6. Y. Grossman and H.R. Quinn, Phys. Rev. D **58**, 017504 (1998)
7. R. Aleksan, I. Dunietz, B. Kayser, and F. Le Diberder, Nucl. Phys. B **361**, 141 (1991).
8. *BABAR* Collaboration, B. Aubert *et al.*, SLAC-PUB-9310, hep-ex/0207063; SLAC-PUB-9304, hep-ex/0207065; SLAC-PUB-9303, hep-ex/0207068.
9. The *BABAR* detector is described in B. Aubert *et al.*, Nucl. Instr. and Methods A **479**, 1 (2002).
10. *BABAR* Collaboration, B. Aubert *et al.*, SLAC-PUB-9060, hep-ex/0201020, to appear in Phys. Rev. D **.**
11. BELLE Collaboration, B.C.K. Casey *et al.*, hep-ex/0207090, submitted to Phys. Rev. D **;** CLEO Collaboration, D. Cronin-Hennessy *et al.*, Phys. Rev. Lett. **85**, 515 (2000); CLEO Collaboration, S. Chen *et al.*, Phys. Rev. Lett. **85**, 525 (2000).
12. Particle Data Group, K. Hagiwara *et al.*, Phys. Rev. D **66**, 010001 (2002).
13. Belle Collaboration, K. Abe *et al.*, Phys. Rev. Lett. **89**, 071801 (2002).